Modeling methodology for the accurate and prompt prediction of symptomatic events in chronic diseases

Josué Pagán[a,b,*], José L. Risco-Martín[a], José M. Moya[c,b], José L. Ayala[a]

[a]Dpt. of Computer Architecture and Automation, Complutense University of Madrid, Madrid 28040, Spain
[b]CCS-Center for Computational Simulation, Campus de Montegancedo UPM, Boadilla del Monte 28660, Spain
[c]LSI-Integrated Systems Laboratory, Technical University of Madrid, Madrid 28040, Spain

Abstract

Prediction of symptomatic crises in chronic diseases allows to take decisions before the symptoms occur, such as the intake of drugs to avoid the symptoms or the activation of medical alarms. The prediction horizon is in this case an important parameter in order to fulfill the pharmacokinetics of medications, or the time response of medical services. This paper presents a study about the prediction limits of a chronic disease with symptomatic crises: the migraine. For that purpose, this work develops a methodology to build predictive migraine models and to improve these predictions beyond the limits of the initial models. The maximum prediction horizon is analyzed, and its dependency on the selected features is studied. A strategy for model selection is proposed to tackle the trade off between conservative but robust predictive models, with respect to less accurate predictions with higher horizons. The obtained results show a prediction horizon close to 40 minutes, which is in the time range of the drug pharmacokinetics. Experiments have been performed in a realistic scenario where input data have been acquired in an ambulatory clinical study by the deployment of a non-intrusive Wireless Body Sensor Network. Our results provide an effective methodology for the selection of the future horizon in the development of prediction algorithms for diseases experiencing symptomatic crises.

Keywords: migraine, WBSN, modeling, state-space, identification, prediction, feature

1. Introduction

Currently, there exists a growing interest in the use of Wireless Body Sensor Networks (WBSNs) as an effective mechanism to monitor biometric signals. These networks are good candidates for the monitorization of chronic diseases because they are fully portable and non intrusive. The monitorization process enables the study of diseases, and also the prediction of critical events related to the disease during the monitorization period. These networks have become more popular with the development of high-performance embedded architectures and the improvement of their battery life. As pointed out in [1], many applications and possibilities emerge in areas such as healthcare for the elderly, remote medical diagnosis, disease alarm notifications [2] or mobile applications for sport training [3]. The deployment of these WBSNs involves the management of large medical databases, and the development of various processing techniques. For example, data mining techniques [4] applied to data acquired by wearable systems allow the detection and classification of epileptic seizures, as Heldberg *et al.* do in [5].

Algorithms for modeling and prediction have also been proposed in some medical areas. There are many pathologies that can benefit from predictions, such as those presenting symptomatic crises. A symptomatic crisis is defined as the manifestation of the symptoms of a disease. Many diseases present symptomatic crises, like strokes, epileptic seizures, migraines, psychiatric pathologies or even digestive pathologies. In some cases, prediction of a symptomatic crisis is crucial for the patient—for example, prediction of heart attack in cardiovascular diseases [6].

Many chronic diseases with symptomatic crises exhibit changes in the biosignals regulated by the Autonomic Nervous System (ANS). Some examples of

---
*Corresponding author
Email addresses: jpagan@ucm.es (Josué Pagán), jlrisco@ucm.es (José L. Risco-Martín), josem@die.upm.es (José M. Moya), jayala@ucm.es (José L. Ayala)

diseases with affection in the ANS are multiple sclerosis [7], Parkinson disease [8] or cluster headaches and migraines [9].

ANS controls the hemodynamic signals like body temperature, electrodermal activity or heart rate. These signals are easily monitorized in an ambulatory and non-intrusive way, such as ECG or the body temperature [10]. We understand as ambulatory monitorization the process that does not require to be conducted in hospital, i.e., the patients can continue their normal activities. For the easy and comfortable monitorization of these signals, we can deploy WBSNs.

The aforementioned predictions of symptomatic crises are sensitive to the prediction horizon (i.e. the time between declaration of an hypothetical event and the event itself). Time response between prediction and the event is a critical period to take decisions, such as activating a medical alarm or notifying the intake of a drug.

The prediction horizon is a critical parameter. This paper presents a study of the effectiveness of prediction in the detection of a symptomatic crisis. Additionally, we will present how our study can be applied in a real case of a chronic disease, the prediction of migraines. This case study has been selected because of the complexity of the problem in terms of modeling and variable selection, as well as its social-economical impact.

It is known that several hemodynamic variables change regulated by ANS when a migraine occurs. ANS regulates hemodynamic variables such as the heart and respiratory rate or sweating and vasomotor activity. This also happens in migraines. Some previous works on migraine treatment have demonstrated that, with the usage of domperidona and naratriptan, the earlier the intake of the medication, the more effective is. Goadsby *et al.* show some results in [11]. There are studies about the usage of other triptans with a shorter time of actuation. In the same line, in [12] it is shown that the pharmacokinetics of specific migraine treatments, such as rizatriptan or sumatriptan, can abort migraines in 30 and 10 minutes respectively. Therefore, any prediction of the migraine crisis would be extremely useful to avoid the pain before its onset, as the pharmacological treatment already exists.

Some of the migraineurs (defined in the clinical terminology as the people suffering from migraines) have their own prediction flags such as aura (perceptual disturbance experienced by the patient before the pain) or prodromic symptoms (subjective and unspecific perceptual disturbances). However, these symptoms can appear at any time from 48 to 6 hours before the onset of the migraine, discarding these as good predictors. Our hypothesis is the following: if we understand the changes that happen to the hemodynamic variables, we could predict the onset of a migraine. If the prediction time is long enough to reach the times of the pharmacokinetics of the drugs, we could anticipate the intake of these to abort the migraine.

The aim of this paper is to propose a methodology to show the limits of prediction of symptomatic crises using state-space models. The main goal of this work is not in the prediction itself, that has been already proved by the authors, but in the mechanisms applied to increase the accuracy of predictive models by tuning their parameters. In this paper, we also show how predictions can be improved by removing spurious and noisy data in the input data set. Predictive algorithms frequently applied in the literature to static datasets [6, 13], where there is no data loss and signals are less noisy. This study will use real data gathered from a WBSN, that imposes severe constraints in the processing of noisy and unreliable data. Thus, the proposed methodology will study the best options for prediction according to the availability or status of sensors and the desired horizon using data from a real ambulatory study.

The remainder of this paper is as follows. Section 2 explains the methodology followed to gather the data and its management, as well as the description of the parameters used in the algorithms envisioned to solve our problem. Section 3 shows the results obtained and their discussion. Finally, some conclusions of this work are drawn in Section 4.

2. Methods

This work presents a methodology to improve prediction models for chronic diseases with symptomatic crises. It also analyzes the prediction limits when applied to a real case study of a chronic disease with symptomatic crises, the migraine. Due to the complexity of an ambulatory study like the one presented in this paper (recruitment of patients, deployment of a large number of monitoring devices, long monitorization time, etc.), this work is focused only on the migraine disease. In the opinion of the authors, the methodology presented in this work is fully applicable to other chronic diseases drawing subjective pain symptomatic curves. The diagram
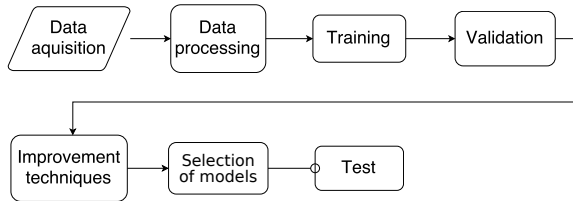
Figure 1: General overview of the proposed methodology.

Table 1: Data acquisition parameters.

	Placement	Sampling (Hz)	Precision	Data-24h (KB)
TEMP	Armpit	1	0.0223 °C	126.6
EDA	Arm	1	0.0062 μ S	126.6
ECG (HR)	Breast	250 (0.1)	4 ms (1 bpm)	31640.6 (12.7)
SpO2	Finger	3	1 %	253.1
	Total (MB)			31.4 (0.51)

in Figure 1 presents an overview of the steps of the proposed methodology.

Firstly, Section 2.1 relates the main characteristics of the data used and the developed processing techniques. Next, training and validation of the models are shown in Section 2.2. Finally, a very critical block of our methodology is presented: the development of improvement techniques, shown in Section 2.3. These techniques will be applied after obtaining the predictive model, in order to increase the accuracy and the horizon length. Results obtained by our techniques support the importance of deriving a methodology like the one proposed in this paper.

2.1. Data

Four hemodynamic variables have been monitorized in migraineurs during 24 hours per day: heart rate (HR), electrodermal activity (EDA), skin temperature (TEMP) and peripheral capillary oxygen saturation (SpO2). A multivariable analysis of these signals is applied to predict a migraine crisis. In addition to the hemodynamic variables, the subjective pain has been manually registered by patients to correlate the real pain with the biometric signals and to train the predictive models.

Changes in these hemodynamic variables regulated by ANS are related in the clinic literature to the migraine. For instance, Hassinger *et al.* relate the cardiovascular response to the migraine [14] and Vollono *et al.* do the same with the heart rate variability during the sleep [15]. Kewman *et al.*, for example link changes in the skin temperature with migraines, as other authors do [16]. In a previous study, these variables have demonstrated to be good predictors of the migraine [17]. Passchier shows also changes in the electrodermal activity in migraine sufferers in [18]. Regarding the SpO2, Lovati shows in [19] how blood oxygenation during sleep was significantly higher among headache patients with respect to controls.

Once the patients have signed the informed consent (the protocol for the clinical study that was approved by the Local Ethics Committee of the hospital), the monitorization phase begins. Two sensing motes are used: i) PLUX-Wireless Biosignals [20] to acquire EDA, skin temperature and ECG signals, and ii) Nonin Onyx II [21] to acquire SpO2. Table 1 summarizes the placement of sensors, their data acquisition rate, accuracy, and the amount of data gathered during 24 hours of monitorization. Despite the HR is used for modeling, this is calculated offline from the ECG signal; this fact reduces the amount of data to process from 31.4 MB to 0.51 MB per day.

Patients indicate through an electronic form in an Android smartphone the beginning and the end of the symptomatic crisis. They also mark the relative changes in pain intensity or punctual pain levels during the migraine crisis (several marks during the migraine). These relative changes are not limited in a numbered scale [17] (from $-2^{32} + 1$ to $2^{32} - 1$). In addition, patients mark a global pain that defines the whole migraine, this time in a normalized and limited scale 0–10 [22], in order to verify that the crisis corresponds to a migraine or another kind of headache. The two sensing motes send the data to the smartphone via Bluetooth and then the data are transmitted to a Cloud storage system. Data processing as well as optimization and predictive algorithms run on a remote PC or server.

The punctual relative pain levels indicate the subjective pain intensity. The maximum represents the highest pain, and it will be different for each migraine and patient. Patients do not know if their current pain is the maximum or not. Hence, the use of an unlimited scale allows marking high values to prevent saturation. Each curve is normalized (0 to 100%) and modeled as two semi-Gaussian curves. These curves have shown a good fit to the points marked by the patients. The parameters necessary to define such symptomatic curve are $\{(\mu_1, \sigma_1), (\mu_2, \sigma_2)\}$ [17]. The symptomatic curve includes the aura (if it exists) because it reflects some changes in the migraine process and this is considered a symptomatic process. An example is shown in Figure 2.
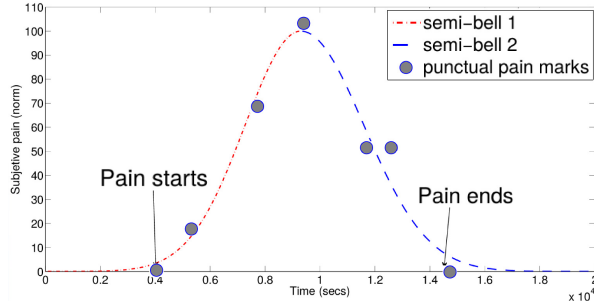
3

Figure 2: Modeling of subjective pain evolution curve.

Signals are synchronized before running the algorithms. After that, in order to recover disruptions in data, a Gaussian Process Machine Learning (GPML) procedure is followed. This process is based on the work developed by Rasmussen [23] and their tool [24]. Signals are synchronized, and the disruptions in the data are repaired using a Gaussian likelihood function by GPML. The normalized root mean square error (NRMSE), also called fit, is the metric used to calculate the goodness of the fitting of GPML with the available data (some data are lost during transmission because sensors can disconnect or the wireless transmission link is noisy). The fit is defined as:

$$ fit = 100 \times \left(1 - \frac{\|y - \hat{y}\|}{\|y - mean(y)\|} \right) \qquad (1) $$

where y is the real (Gaussian modeled) symptomatic curve, and $\hat{y}$ is the predicted one.

After the synchronization, the time between samples is set to 1 minute for all signals. Figure 3 shows the four hemodynamic signals during an asymptomatic period (green lines) and a migraine event (red lines between vertical bars) in the middle. These data have been synchronized and repaired using the GPML. The average fit achieved for all the signals in Figure 3 using the GPML is 81.9%.

For this paper, in order to show results for the methodology proposed in Section 2.3, data from two patients have been selected from the monitoring database (labeled as Patient A and B). Data from Patient A correspond to a young female patient that suffers from migraines with aura and does not undergo medical treatment. 20 migraines have been acquired in two different experimental periods (nearly one month each). Data from Patient B correspond to a middle aged female patient that suffers from migraines without aura and undergoes preventive medical treatment. 12 migraines have been acquired in one experimental period (almost a month). The training dataset for Patient A and B was of M=15 and M=8 randomly chosen migraine events, respectively.

2.2. Models

It is well known that migraines are a sequence of neurological stages: i) prodromic symptoms, ii) aura phase, iii) the pain itself and iv) finally a postdromic stage [25]. As aforementioned, the intake time of the drugs used to stop the symptoms of the migraine is of critical importance. The earlier the intake, the more the effectiveness, because when the pain cycle begins, there is an activation of the trigeminal nucleus and it is much more difficult to stop it [11]. Thus, the success of the medicine to stop the pain strongly depends on the prediction horizon; hence, a methodology to achieve the maximum prediction horizon is needed.

The N4SID state-space algorithm [26] has been chosen for its accuracy in modeling other biomedical processes, such as Cescon presented in [27] or Facchinetti in [28], both studies about diabetes. N4SID models have been used in other previous works in the literature of bioinformatics applications, reaching good results. For instance, to estimate infections in populations, like Tan *et al.* did in [29] for HIV, or Hooker *et al.* did in [30] for infectious diseases. The N4SID algorithm has shown also good results in the biomedical area as detector of anomalies in the electrocardiogram signal, as Munevar *et al.* demonstrate in [31].

In this work, the N4SID algorithm has been computed using the System Identification Toolbox of the MATLAB software [32].

2.2.1. Training the models

A state-space model is a mathematical representation that describes an output (or multiple outputs) as the relation of a set of inputs and state variables by difference equations. These states are immeasurable. The current and future outputs are related, through the system, with past and current inputs. The N4SID is a stochastic model, represented in the general form as a multi-input multi-output (MIMO) linear time-invariant system (LTI) [33] as in Eq. 2:

$$ \begin{aligned} x_{k+1} &= Ax_k + Bu_k + w_k \\ y_k &= Cx_k + Du_k + v_k \end{aligned} \qquad (2) $$

In our case, u_k are 4 hemodynamic inputs and y_k is 1 output (pain level), both at time step k. A is the state transition matrix and relates the next state (x_{k+1}) to the current one (x_k); B relates the next state to the current inputs (u_k); C relates the current state to the current
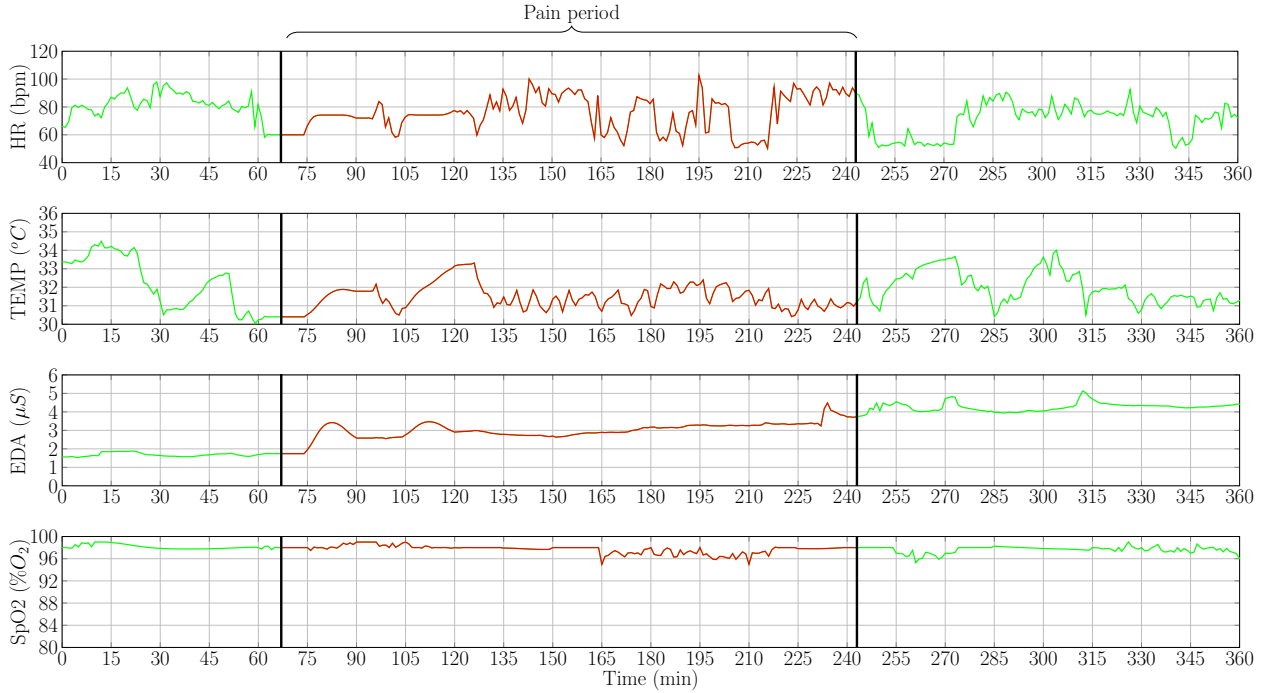
4

Figure 3: Hemodynamic variables after synchronization and preprocessing during a migraine episode (red curve between vertical bars).

output (y_k), and D equals zero in our case. v_k and w_k are immeasurable white noises.

The metric used to evaluate the accuracy of the models is the aforementioned fit. In the training process, the N4SID order nx (size of the square matrix A) and the number of samples from the past inputs and the output are chosen by the algorithm as the ones that achieve the best fit. To do this, the process runs in a triple loop looking for the best parameters. The inner loop chooses the order of the models. The one in the middle chooses the backward window to get information from past inputs. The outer loop only fixes the prediction horizon as shown in this pseudo-code:

```
prevFit = -Inf; %Previous fit achieved

% For six future, sixty past horizons and ten orders
for futWin = 10:10:60
  for pastWin = 0:5:120
     opts = n4sidOptions(futWin, pastWin);
     for nx=1:10
        % Calculate the model
        stateSystem = n4sid(data, nx, opts);

        % Calculate the fit
        fit = compare(data, stateSystem, futWin);

        if fit > prevFit
           % Paremeters of the current best model
           prevFit = fit;
           bestPast(futWin) = pastWin;
           bestOrder(futWin) = nx;
        end
```
```
      end
   end
end
```

In addition, a parallel study for feature selection has been performed. Models have not only been trained with four hemodynamic inputs, but also with the combinations in triads of them; in total, we checked 5 sets of features. From these experiments, we will obtain the features that better describe a migraine per patient.

After training the models, 240 combinations are checked to select the best one per future horizon and per migraine event, and per set of features.

2.2.2. Validation of models

In the validation process, we look for the best models to predict migraines using the cross-validation criteria: each model M_i, $i = 1, 2, \ldots, M$, obtained from the i-th migraine is validated against the other j-th migraines, with $i \neq j$. The validations are performed for the same horizon for which the model was trained. We compare two models M_i and M_j regarding their average fit. The average fit of each model is calculated from the $M - 1$ validation. The better the average fit in validation, the better the model.

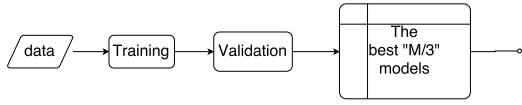A model is considered good when it is able to

5

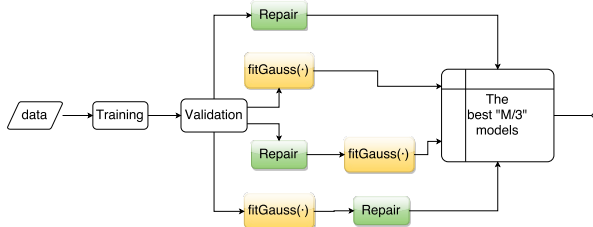Figure 4: Basic scheme to select the best models for each patient.

Figure 5: Schemes proposed to be used in the methodology.

validate at least $\lceil M/3 \rceil$ of the migraines from the dataset at a given fit. More than one model is selected in order to calculate an average prediction and to avoid any bias. The criterion followed is to select the best $\lceil M/3 \rceil$ models trained. Figure 4 represents the basic scheme of training and validation. The last module in the figure represents the model selection that implements the proposed methodology.

2.3. Improving results

This block, from the scheme shown in Figure 1, implements a sequence of processes to improve the prediction. The predictions obtained by the N4SID models have difficulties maintaining a constant value, and they tend to oscillate around the zero value when no symptomatic crisis is detected. This fluctuation causes an artificial reduction in the fit. The blue curve in Figure 6a represents a prediction with fluctuations (the original symptomatic curve is the black one). These oscillations can be easily detected and removed. To do this, two methods are evaluated: i) reparation of the prediction, and ii) Gaussian fitting as the original symptomatic crisis was modeled. These methods are applied to the basic scheme of Figure 4. All the possibilities studied are shown in Figure 5. Each one of the four branches represents a scheme to improve the predictions.

2.3.1. Reparation of the prediction

In order to illustrate these processes, Figures 6a and 6b show how to repair a prediction. False positives are detected using a level and a time threshold. Firstly, those values out of limits (below zero and above the maximum) are marked with red x,

as shown in Figure 6a. Then, negative values are set to zero, and the rest of outliers are set to the maximum. After that, the level threshold is applied. This process marks as detections those values above 50% of the probability of occurrence (green circles in Figure 6a), using the linear decider explained below. The 50% of pain probability is projected to a level of 32 over the ideal prediction (same as the original symptomatic curve). The blue dotted line represents this in Figure 6b and extends through Figure 6a.

Finally, the time threshold is applied. If the distance between the farthest points is lower than 60 minutes (enough to detect if a migraine attack occurs or not), it is considered as a false positive. These points are removed. In Figure 6a the left detection is removed.

As a result, the repaired prediction is represented in Figure 6c (purple curve). It is worth noting that the fluctuation that appears in the middle of the curve was not detected by the threshold level.

In the following, we present how the linear decider works. The use of this decider was initially introduced in a previous work [17], and here we summarize the main characteristics to help the reader to understand the next stages of this research.

The linear decider will detect a migraine event when the probability of occurrence of a detection exceeds the 50% of probability. This linear decider (blue triangle in Figure 6b) ranges from 0% (minimum pain intensity in the normalized symptomatic Gaussian curve) to 100% (maximum pain intensity in the normalized symptomatic Gaussian curve) of probability (see Section 2.1). Therefore, the linear decider projects the repaired prediction (blue signal in Figure 6a) to a probability of occurrence curve (green curve in Figure 6b). The linear decider uses a linear function as the projection function. As a result, the migraine detected (all those values higher than the 50% of probability of occurrence) is bounded by the red dotted line in Figure 6b.

2.3.2. Gaussian fitting

Figure 6c also illustrates the result of applying the Gaussian fit (orange curve). This process fits the prediction to two semi-Gaussian curves, with reference at the maximum of the prediction. With the aim of finding the original bells, the prediction is first normalized and then fitted.

The impact of the combination of both processes (repair and Gaussian fitting, depicted in the two lower branches of Figure 5), is also analyzed in Section 3.
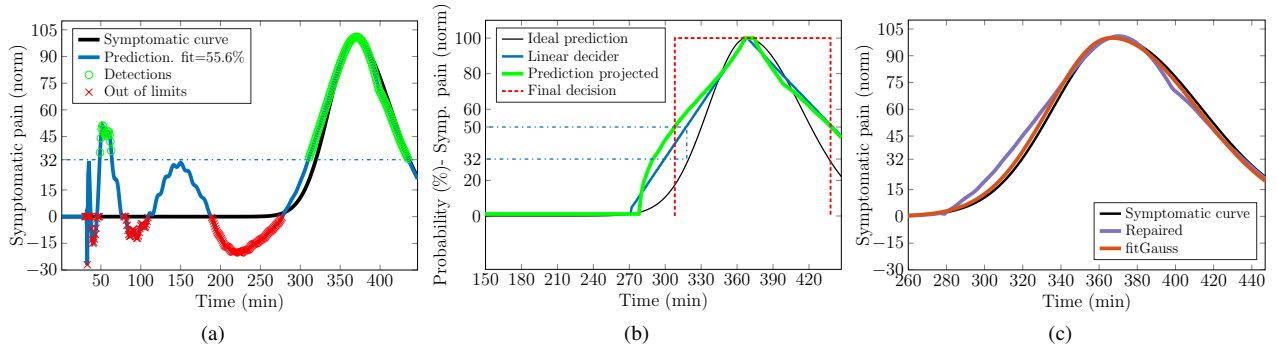
Figure 6: Improving the predictions. (**a**) Prediction over real symptomatic curve. Detection of events, removal of oscillations and false positive detected; (**b**) Probability curve of pain occurrence from the repaired prediction over the ideal probability curve. Final detection time limits; (**c**) Result after repairing the prediction and fitting the prediction to two semi-Gaussian curves.

2.4. Fitting and prediction criteria

The goodness of the fit and the prediction horizon can be used as criteria to select the models. Selecting one criterion automatically sets the other. Setting the fit, we can follow a more conservative approach that reduces the prediction horizon but improves the confidence in the models. However, setting the prediction horizon can achieve farthest predictions by loosing accuracy. In the following section, we choose first a minimum fit as requirement for the model selection. Later, a strategy is shown to select the models according to the prediction horizon.

A fit of 70% has been selected as the threshold of similarity to consider a model as good candidate.

3. Results

In this section we present the experimental results obtained by our proposed methodology, designed to enlarge the prediction horizon of predictive models for symptomatic crises. As stated before, this method has been tested with N4SID, a well-known state-space based algorithm. Firstly, we present the results of model training. Secondly, we show the validations of these models, where all the improvement schemes presented in Figure 5 are studied. Finally, one scheme is selected and the models are tested with new signals (migraines not used in the training and validation sets).

Along this section, our criterion has selected a 70% for the fit value. This is a conservative setup that will improve the confidence in the models (see Section 2.4). The alternative approach (to set the prediction horizon by loosing accuracy) is also tested in Section 3.4.

3.1. Training the models

As mentioned in Section 2.2.1, each migraine has been trained for 6 different horizons and 5 different feature combinations. Figures 7a and 7b summarize the training results for patients A and B respectively. Each value on the surface of these graphs represents the average of fits over all the trained models (M = 15 models for Patient A, and M = 8 for Patient B). For Patient A, the fit decreases more quickly than for Patient B. In addition, the training results for patient B are almost 15-20 points higher than the results for Patient A. This can be explained by the higher amount of data lost during monitorization of Patient A (in spite of the usage of GPML).

In Figures 7a and 7b, maximum fits are reached for lowest horizons (10 and 20 minutes). The fit decreases with the horizon, but also depends on the features selected. The highest values of fit are reached for the combination of the four available biometric variables. It is worth to mention that a valley is found around the prediction horizon of 40 minutes. Surprisingly, this occurs for the TEMP-HR-SpO2 feature combination in both patients. As the number of individuals is not enough, this should not be considered as a conclusion. At this point, the fit for Patient A is 73.2%, and 94.8% for Patient B. This suggests that the time window for prediction is larger for Patient B than for Patient A. Additionally, fits increase with prediction horizons larger than 40 minutes (50 and 60 minutes); this is due to overfitting during training (see Section 3.2). It seems that our modeling approach in the training stage reaches the limit for the migraine prediction at 40 minutes.

Table 2 shows the training results for each model for patients A and B. This table summarizes the fit reached
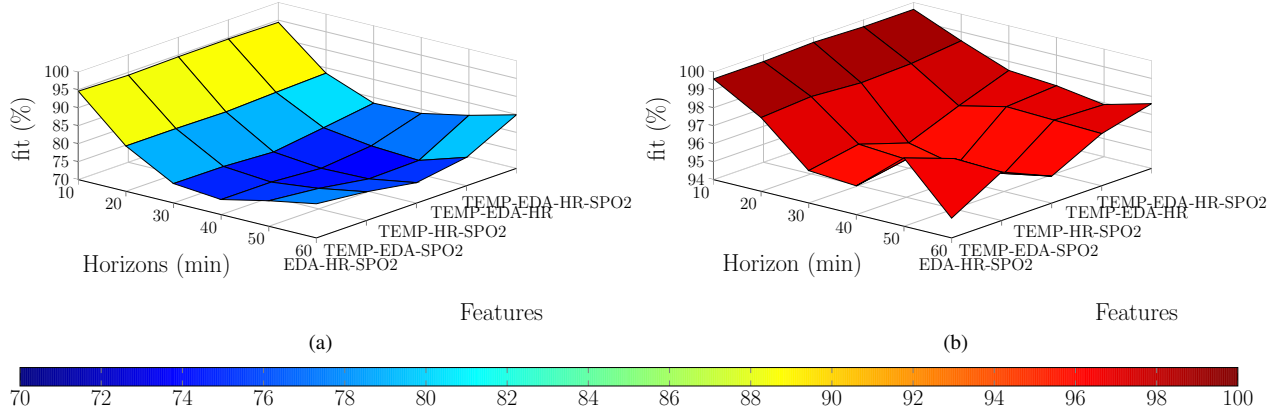
Figure 7: Average fits for training. Dependence with the future horizon and selected variables. (**a**) Data from Patient A; (**b**) Data from Patient B

Table 2: Training results for the TEMP-EDA-HR-SpO2 features set and 40 minutes forward horizon for patients A and B.

	Patient A															Patient B							
	M_1	M_2	M_3	M_4	M_5	M_6	M_7	M_8	M_9	M_{10}	M_{11}	M_{12}	M_{13}	M_{14}	M_{15}	M_1	M_2	M_3	M_4	M_5	M_6	M_7	M_8
$fit(\%)$	84,4	84,1	88,1	75,6	70,6	85,0	86,7	**65,8**	78,9	82,6	79,2	**67,4**	80,8	81,0	72,0	97,5	99,6	95,9	99,5	90,0	97,0	99,9	98,1
ph (min)	25	105	60	40	30	30	70	75	15	100	60	95	20	105	90	12	30	14	20	25	25	15	18
nx	6	4	7	8	5	9	5	6	10	9	7	8	7	4	7	6	9	7	6	10	8	10	9

by the models, the past horizon (*ph*, in minutes) required to train them, and the order of the matrices required to reach the best fit. For the sake of space, only results for the horizon of 40 minutes and for the TEMP-EDA-HR-SpO2 combination of features are shown. This setup corresponds to the minimum training error. The fits are 78.8% and 97.2% in average for patients A and B, respectively.

As can be seen, fits reached are high for both patients, and they are always over 70% (except for two Patient A cases marked in bold in Table 2). However, models require large matrices (larger than order $nx = 7$) in most of the cases. Despite the high orders, past horizons are low for Patient B (they are always lower than 30, 20 minutes in average); but they are high for Patient A (61 minutes in average and up to 105 minutes backward). For the remaining future horizons and feature sets, the average fit in training keeps high, always over the 70% for both patients. No correlation has been found between the order of matrices and the number of past inputs.

In (Section 3.2) we present the results for model validation. Here, trained models are tested as predictors of the other symptomatic crises of the training dataset. In the following section, we will also analyze the overfitting effect.

3.2. Validations of models

In this section we show the results of performing cross-validation between models, as mentioned in Section 2.2.2. The main objective of this section is to discard overfitted models. In this way, we will find those models that reach the longest prediction horizon. Results have been obtained for the 6 different prediction horizons and the 5 feature combinations.

Table 3 represents the number of useful models with average fit over all the cross-validations exceeding 70%. As the average prediction is calculated over more than one model, this analysis will help on the selection of the models. It is considered that, at least, one third of the models must validate with high average fit to choose a feature set as relevant (for each prediction horizon). According to the results in Table 3, no difference appears between the selected features for a forward horizon of 10 minutes. In general, no model is able to validate for higher horizons than 20 and 30 minutes for patient A and B respectively. This confirms that the valley in training in Figures 7a and 7b marks the limit of prediction for state-space models, and models trained over 40 minutes are overfitted.

The four-features combination is always the worst combination. For Patient A and 20 minutes forward horizon, the combinations of three features, except for TEMP-HR-SpO2, show 5 available models (in the limit

of our criterion to consider the features as relevant). For Patient B, all the combinations of features look good (more than 3 models over the average fit of 70% in this case) for 20 minutes, but only the TEMP-HR-SpO2 feature combination is useful for 30 minutes.

Table 3: # Useful models after validation.

	Patient A						Patient B					
Features / Horizon (min)	10	20	30	40	50	60	10	20	30	40	50	60
TEMP-EDA-HR-SpO2	15	4	0	0	0	0	8	4	1	0	0	0
TEMP-EDA-HR	15	5	0	0	0	0	8	6	1	0	0	0
TEMP-EDA-SpO2	15	5	0	0	0	0	8	6	2	0	0	0
TEMP-HR-SpO2	15	7	0	0	0	0	8	7	4	0	0	0
EDA-HR-SpO2	15	5	0	0	0	0	8	7	1	0	0	0

As aforementioned in Section 3.1, high fits in training do not assure good models, and some of them must be discarded in the validation phase.

As the 20 minutes prediction horizon seems to be the safest horizon, we use this to show the results for Patient A in Figures 8a through 8e and for Patient B in Figures 9a through 9e. Horizontal axes in these figures represent each one of the validated models. Vertical axes represent the average fit achieved, obtained as the average of the $M - V_{ov} - 1$ validations. The whiskers represent the standard deviation, σ. V_{ov}, are the overfitted validations (negative fit). These were removed to calculate the average. The red line indicates the threshold set as fitting criterion.

The deviations (the whiskers) for validations in Patient B (σ_B) are lower than deviations in Patient A (σ_A). This means that, the confidence of models from Patient B should be higher than from Patient A. We can also state that these models are more generalizable because the results for Patient B are more consistent than those for Patient A, as data acquired from Patient B have less discontinuities during monitorization.

Regarding the average values in Figures 8a through 8e, as the four-features combination is a poor election, only 4 models have an average fit higher that 70%. For the TEMP-HR-SpO2 combination of features (Figure 8d) we achieve the best results. In this case, 7 models exceed the threshold of 70%. Something similar occurs with the results for Patient B.

As aforementioned, to calculate the average fit, validations with negative results have been removed. In some cases, the number of useful validations is really low. This happens, for example, with the validation of the model M_9 in Figure 8b, that only validates 3 migraines. The model M_1 for Patient B validates also the same number of migraines in Figure 9a, and only 2 migraines are validated in Figure 9b and Figure 9c

(despite its high fitting).

As a result of the validation study: i) the four-features combination is never the best option to predict migraines for any horizon length, and ii) it seems that 20 minutes forward is the best window to predict migraines for both patients. The first idea means that some biometric variable worsens the prediction in combination with others (but not itself). Hence, by removing one variable we achieve more useful models. The second result achieves a prediction horizon close to the constraints imposed by pharmacokinetics (see Section 1). But, still, we pursue longer prediction horizons and in next Section 3.3 we show how to improve these predictions.

3.3. Improving predictions

This section is devoted to improve the prediction horizon. In this section, the results of the schemes proposed in Section 2.3 for the methodology are shown.

We have studied all the repairing schemes during the validation stage using the four-features combination (TEMP-EDA-HR-SpO2) and the 6 prediction horizons (from 10 to 60 minutes). The F value is used as the metric to compare all the schemes with the basic one (results in Section 3.2, scheme of Figure 4). To compute the F value, the sensitivity (TPR) and the precision (PPV) values are calculated. All values are based on the results of all the $M - 1$ predictions of each M_i model. This means that the true positive (TP) account should be ideally $6 * M * (M - 1)$. The results are shown in Table 4.

Table 4 shows low levels of the F value because it has been calculated as the average of the F values for every horizon. The higher the horizon, the lower the F value, worsening this average F value. The results show a high rate of false positives and low number of detections for horizons higher than 40 minutes, as expected from the training in Section 3.1.

The best scheme for the proposed methodology is the combination of repairing the prediction (remove spurious) and the Gaussian fitting. The order (first repair then fitting) affects more to Patient A than to Patient B. Therefore, the scheme Repair+fitGauss in Figure 5 is chosen as the repairing scheme of symptomatic crises prediction.

Now, the selected scheme is applied and compared with the base scheme. For the sake of simplicity, only the results for Patient B are presented in this section. Figure 10a presents the results of validation for Patient B and all the trained future horizons (10 to 60 minutes
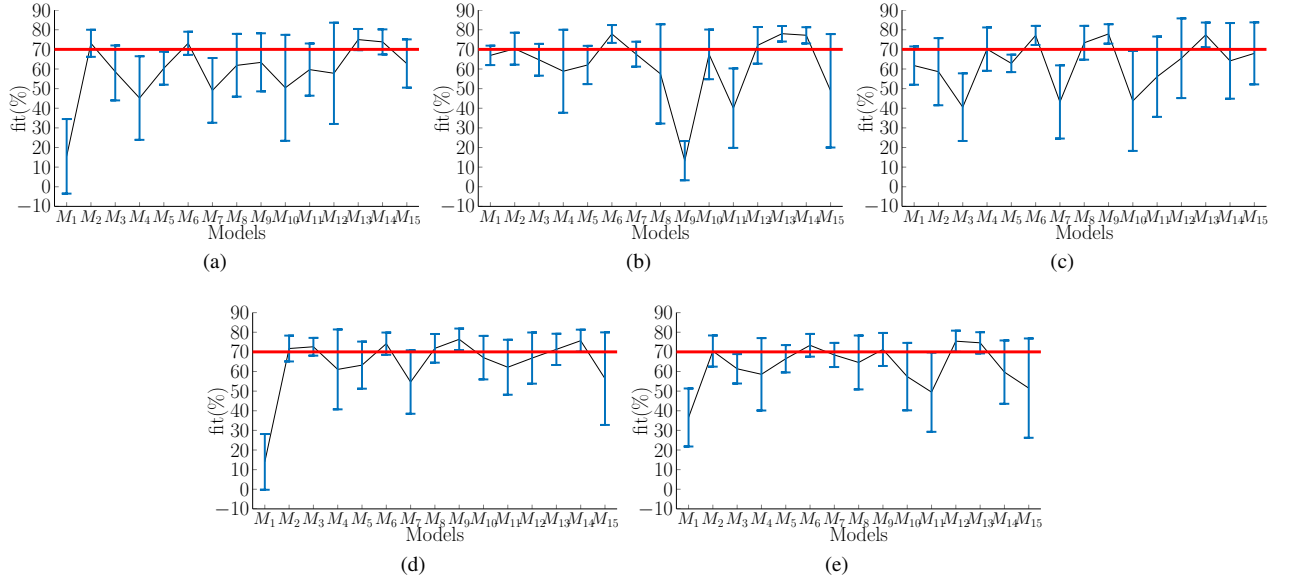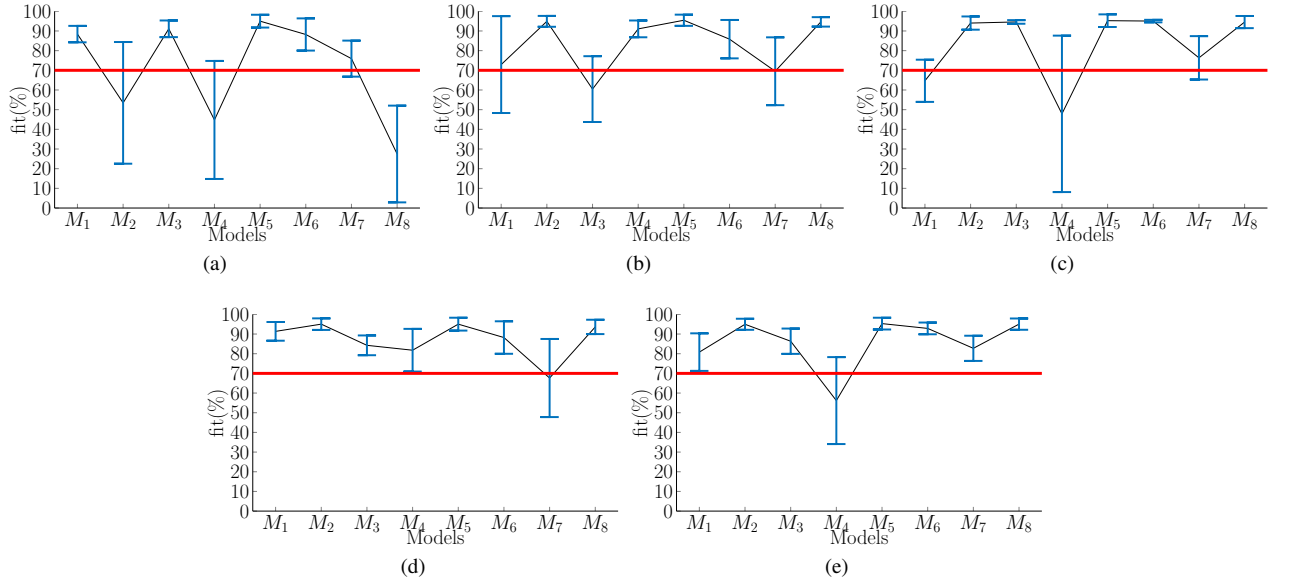
Figure 8: Validation results for models from Patient A. 20 minutes forward horizon. For each features set:(**a**) TEMP-EDA-HR-SpO2; (**b**) TEMP-EDA-HR; (**c**) TEMP-EDA-SpO2; (**d**) TEMP-HR-SpO2; (**e**) EDA-HR-SpO2.

Figure 9: Validation results for models from Patient B. 20 minutes forward horizon. For each features set:(**a**) TEMP-EDA-HR-SpO2; (**b**) TEMP-EDA-HR; (**c**) TEMP-EDA-SpO2; (**d**) TEMP-HR-SpO2; (**e**) EDA-HR-SpO2.

Table 4: F value to compare the schemes proposed for the methodology

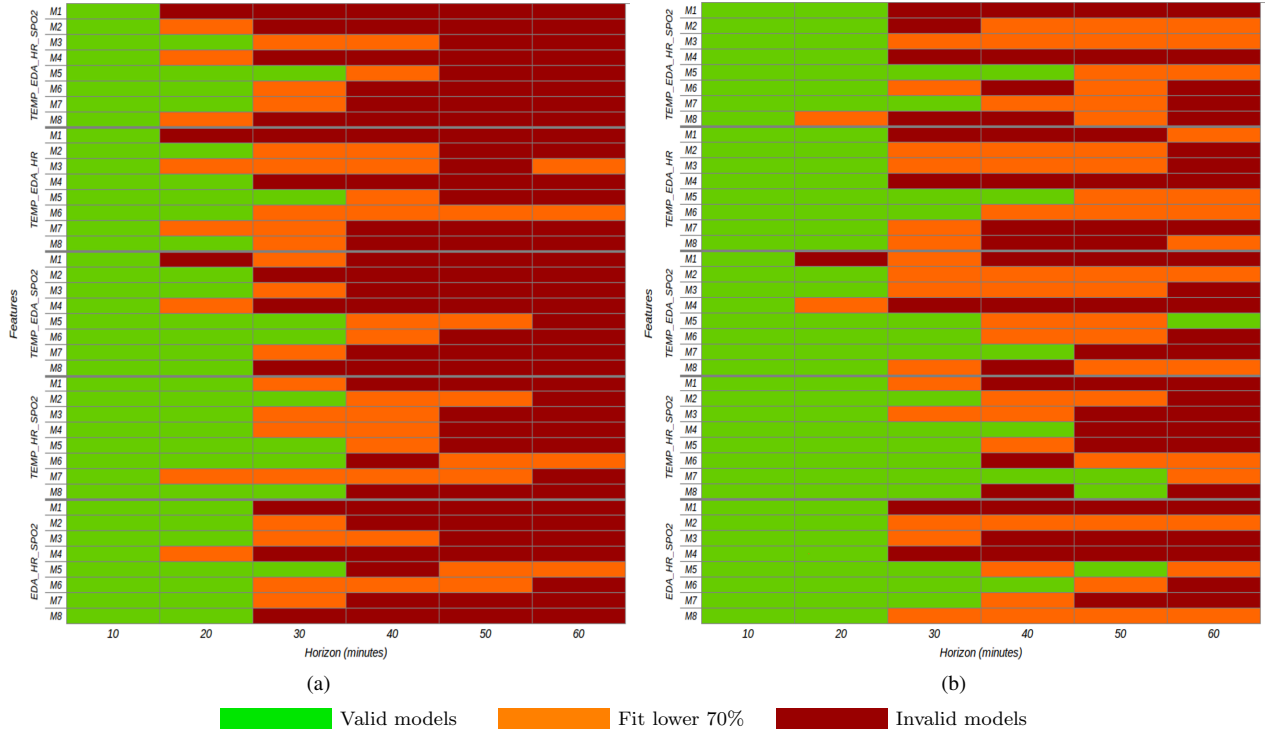|	Base		Repair		FitGauss		Repair + FitGauss		FitGauss + Repair	
	Patient A	Patient B	Patient A	Patient B	Patient A	Patient B	Patient A	Patient B	Patient A	Patient B
TPR (%)	24.7	30.4	29.8	36.3	31.0	39.0	33.1	39.6	30.6	39.0
PPV (%)	45.1	60.7	57.2	90.4	75.1	71.6	80.5	81.1	78.5	87.9
F (%)	31.9	40.5	39.1	51.8	43.8	50.5	46.9	53.2	44.1	54.0

10

Figure 10: Useful models in validation for Patient B at a 70% of fit. (**a**) Without reparation of prediction; (**b**) After reparation of prediction and Gaussian fit.

forward). Horizontal axis represents the six different horizons trained and the vertical axis represents the M = 8 models for each feature combination. Colors represent those models good enough to be used as predictors in a real time implementation (green), those with an average fit lower than 70% (orange) and the discarded ones because the overfitting (red, less than one third of the migraines available are validated).

All models validate all migraines for a prediction horizon of 10 minutes. As aforementioned, for 20 minutes forward almost all models are useful, except model M_1 for some feature combinations. From 30 minutes ahead, there are not enough useful models, except in the TEMP-HR-SpO2 feature combination, where 4 models validate quite well. For prediction horizons equal and greater than 40 minutes, migraine prediction is not possible, as pointed out in Section 3.1 and Section 3.2.

As was introduced in Section 2.2.2, applying repairing techniques to the prediction can increase the prediction horizon. In this case we have applied reparation of the prediction and Gaussian fitting, in this order. This is proved by Figure 10b, again for Patient B. The average prediction horizon has been

incremented in 10 minutes (compared to Table 3), and some models validate migraines with a future horizon equal to 40 minutes. There are improvements in models for most of the prediction horizons and all combination of features. These increments are due to removing false positive detections, negative values, and values higher than the maximum, 100, in the normalized symptomatic pain curve.

Regarding results for Patient A, the improvements achieved have been lower. Although some more models are useful for 20 minutes, no one is useful for 30 minutes of prediction if 70% of fit is expected (validating, at least, $\lceil M/3 \rceil$ of the symptomatic crisis in the training dataset).

As shown, the prediction horizon can be improved applying repairing techniques to the predicted signal, reaching prediction times close to the current time of pharmacokinetics and even exceeding it. Additionally, we have shown a method to test the limits of a given predictive model, that must be applied for each patient individually. In particular, we have found that the maximum prediction horizon for Patient A is in the interval [20, 30] minutes, and in the interval of [30, 40] minutes for Patient B, the same results as in [17].
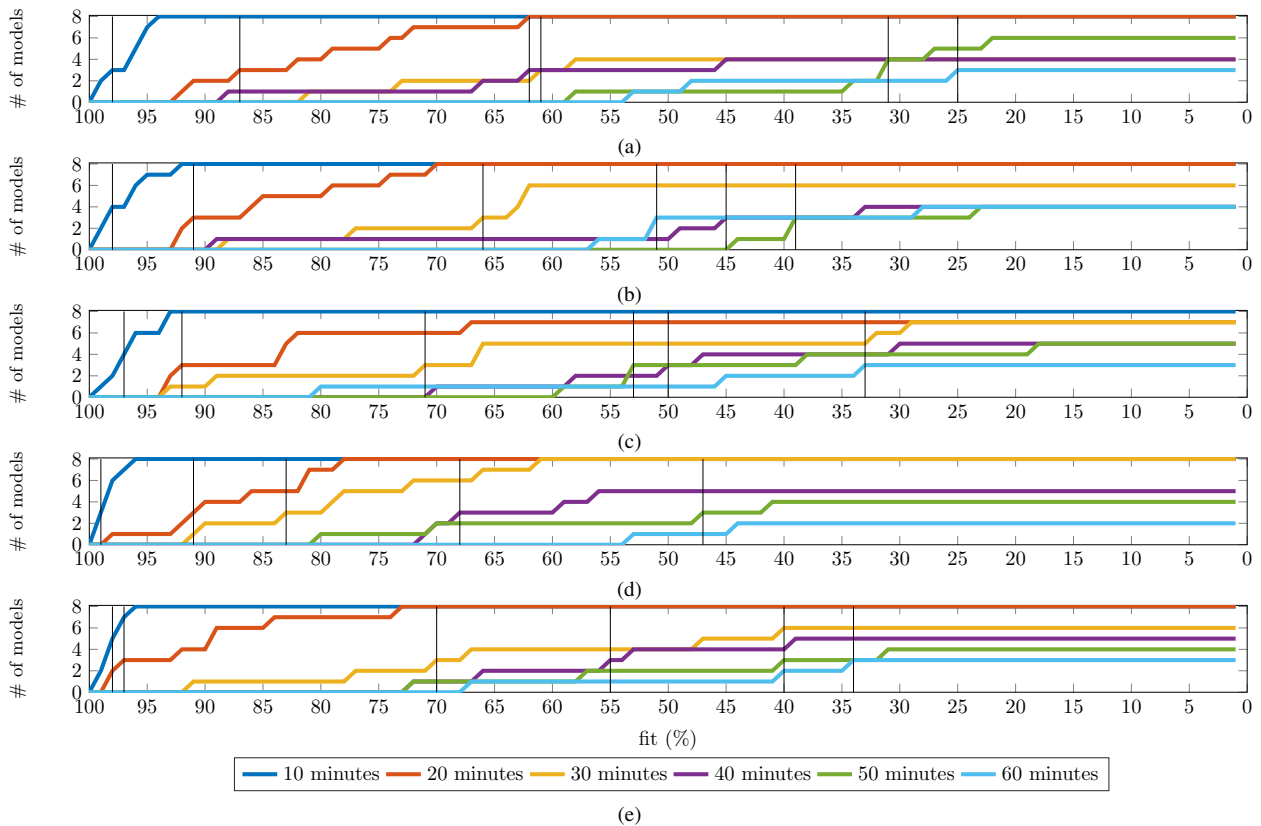
11

Figure 11: Board of strategies for model selection for Patient B. Results after removing the spurious and applying the Gaussian fitting. (**a**) TEMP-EDA-HR-SpO2; (**b**) TEMP-EDA-HR; (**c**) TEMP-EDA-SpO2; (**d**) TEMP-HR-SpO2; (**e**) EDA-HR-SpO2

3.4. Strategy for the selection of models

For the results that have been presented, the fit value has been prioritized, setting a fixed value of 70% and observing the achieved prediction horizon. As mentioned in Section 2.4, in this section we present two different strategies to select the models: i) regarding the fit, or ii) regarding the prediction horizon. In all the cases we always maintain that a model is considered good when it is able to validate at least $\lceil M/3 \rceil$ of the migraines from the dataset at a given fit. The number of migraines to validate are 3 for Patient B (8 migraines available in the training dataset) and 5 for Patient A (15 migraines available in the training dataset). To avoid overfitting and to calculate the average prediction, we still consider as good the selection of, at least, $\lceil M/3 \rceil$ migraines for each feature combination.

Figure 11 shows the number of models available for every horizon at a desired filt level. As a reference, the vertical bars mark the fit where $\lceil M/3 \rceil$ models can predict at least $\lceil M/3 \rceil$ of the migraines in the training dataset. If we focus more on the prediction, i) the first

strategy works setting a desired horizon and looking for the best feature combination that reaches the maximum fit. On the contrary, if we focus more on the fit level, ii) the second strategy works setting a desired fit and looking for the feature combination that reaches the farthest horizon. This is a more conservative selection, for which we set the desired fit or goodness of the prediction and we settle down the available horizon.

For instance, regarding Figure 11, if we are looking for the best prediction horizon 20 minutes forward, we should use the models calculated with EDA-HR-SpO2 in Figure 11e, because the second vertical bar has a higher fit for this feature combination than for the others. There, we find 3 models validating at least 3 migraines each one, in average, with a 97% of fit. But if a prediction of 30 minutes forward is desired, the best option is to select the models using the TEMP-HR-SpO2 feature combination in Figure 11d. For 50 minutes forward we will select the models using TEMP-EDA-SpO2 Figure 11c, and accept only a 50% of fit.

Figure 11 can also be used to look for a desired fit.

For example, if the HR sensor is not available (Figure 11c) and we look for predictions with a fit equal 60% or higher, we could only satisfy a horizon of 30 minutes. On the other hand, if the EDA sensor is not available (Figure 11d), for the same minimum fit of 60% we might predict up to 40 minutes.

It is worth noting that Figure 10b is just a representation of the Figure 11 at 70% of fit. In this figure, we can calculate at 1% of fit how many models that are not able to validate more than 3 migraines still remain.

This methodology leads to a versatile tool for the improvement of predictions and the selection of models for predictions of symptomatic crises in ambulatory real environments. This methodology has been applied in a real clinical study of a disease with high socio-economical impact. The effectiveness of the solution is studied, and the results have proved to meet the pharmacokinetics limits required to avoid the negative effects of symptomatic crises. The results also show that for Patient A the limits of predictions are between 20 and 30 minutes, and between 30 and 40 minutes for Patient B, achieving fits of 70% in both cases.

3.5. Test results

In this section, some test results are shown. Tests have been run using the average model. This is the average of the prediction given by the best $\lceil M/3 \rceil$ models for each feature combination. Over each prediction, as well as over the average of these, the selected improvement scheme has been applied: spurious removal and Gaussian fitting. The test dataset used is: 5 and 4 migraines, and 5 and 6 asymptomatic periods of time for Patients A and B respectively.

A summary of the results is shown in Table 5. As expected, for Patient B, the results of the F value follow the trend of the vertical bars in Figure 11, and the best results are achieved for the feature combination TEMP-HR-SpO2. Best results for Patient A are achieved for the feature combination TEMP-EDA-SpO2. Besides, the worst results are achieved, for both patients, with the combinations of four features. This leads to conclude that the best model selection depends on: i) the features used, ii) the desired horizon or iii) the desired fit.

Our results have been calculated using only data from two patients; therefore, any generalization of the clinical conclusions obtained by this study could be risky. However, the presented methodology, aim of this work, can be validated by these results. In addition, it has been shown that an analysis of the prediction

horizon is needed in order to improve the accuracy of the results, supporting our initial hypothesis.

Figures 12a through 12c shows some test results for Patient A and Figures 12d through 12f for Patient B. Several models applied over different feature sets are presented to show the accuracy of the trained models.

For all the graphs, i) black curves represent the original symptomatic curve that must be predicted, ii) the orange curves are the final result after the reparation of the prediction and the Gaussian fitting.

When a migraine occurs, models provide a prediction of some symptomatic pain levels hours before the pain starts. Nevertheless, these are false positive predictions, and the repairing process removes them. The same happens with negative predictions or those levels higher than 100. For all cases, repairing the prediction and applying a Gaussian fitting leads us to improve the fit. Figures 12c and 12f represent asymptomatic periods of time. The latest present a false positive event not removed, obtained from prediction using the TEMP-EDA-HR-SpO2 feature combination, that presents a high false positive rate. The usage of the board of strategies to select the best models (Figure 11) would have avoided these false positives.

4. Conclusions

The experiments in this paper demonstrate that the use of state-space models to predict symptomatic crises in chronic diseases is time-limited. A methodology is presented as a versatile tool to improve the quality of predictions of these crises, as well as to increase the prediction horizon. This methodology selects models according to the availability of sensors, and according to a desired criteria of fit or prediction horizon. In this work we show how the prediction time window of the disease can be calculated and that it strongly depends on each patient. To prove our methodology, we present a case study for migraine patients. Migraine models have been trained up to 60 minutes in steps of 10 minutes, and it has been demonstrated that state-space algorithms in combination with other techniques (GPML, reparation of prediction and Gaussian fitting of the repaired prediction) are currently limited up to 40 minutes to predict the symptomatic crises of the migraine disease.

Migraines are one of the most disabling diseases, but we have shown how migraine crises can be predicted using WBSNs in an ambulatory way. The prediction horizons found are close or equal to 40 minutes—time enough to predict the migraine pain according to the

Table 5: Test results for Patients A and Patient B at 20 and 30 minutes of prediction horizon respectively at 70% of fit.

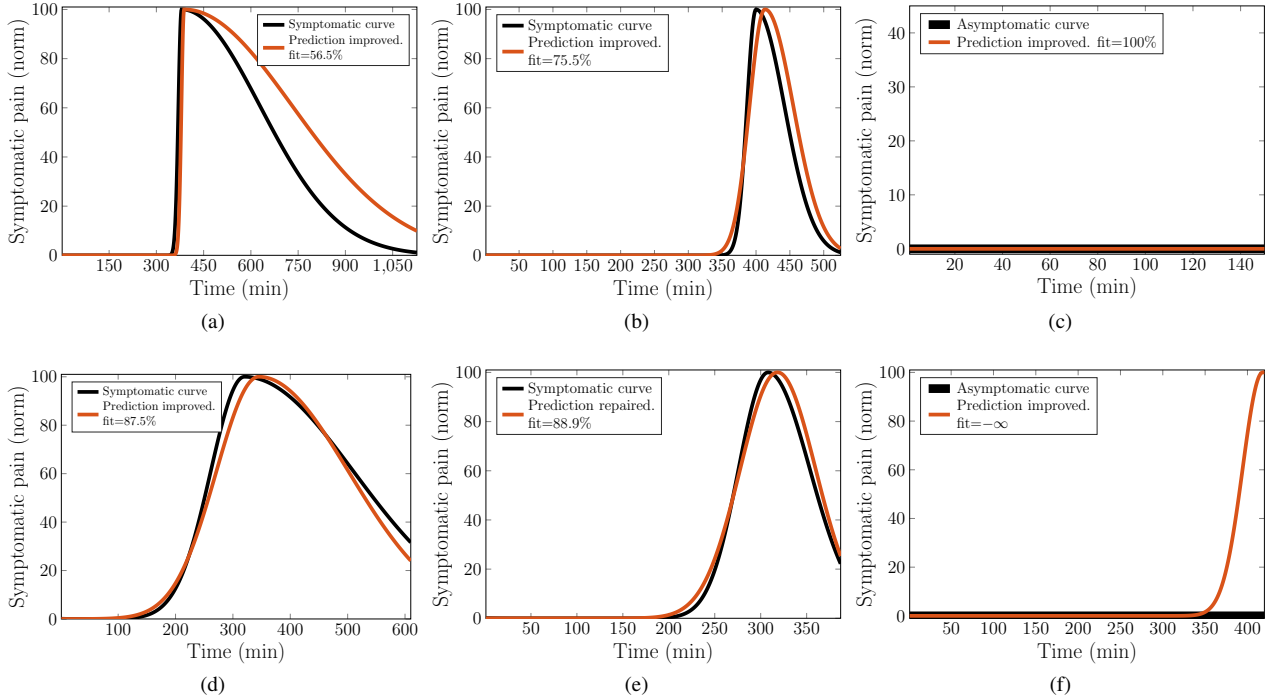|	TEMP-EDA-HR-SpO2		TEMP-EDA-HR		TEMP-EDA-SpO2		TEMP-HR-SpO2		EDA-HR-SpO2	
	Patient A	Patient B	Patient A	Patient B	Patient A	Patient B	Patient A	Patient B	Patient A	Patient B
TPR (%)	50.0	90.0	80.0	100	100	70.0	70.0	100	90.0	40.0
PPV (%)	100	57.1	100	90.0	100	70.0	100	100	90.0	40.0
F (%)	66.7	47.1	88.9	90.0	100	77.8	82.4	100	90.0	47.1

Figure 12: Test results for symptomatic and asymptomatic periods. (**a**) Patient A, TEMP-EDA-HR-SpO2, 20 min forward; (**b**) Patient A, EDA-HR-SpO2, 20 min forward; (**c**) Patient A, TEMP-EDA-SpO2 in an asymptomatic period, 20 min forward; (**d**) Patient B, TEMP-EDA-SpO2, 30 min forward; (**e**) Patient B, TEMP-HR-SpO2, 30 min forward; (**f**) Patient B, TEMP-EDA-HR-SpO2 in an asymptomatic period, 30 min forward.

pharmacokinetics of current treatments—and much more accurate than prodromic symptoms or auras.

Our methodology has proved to be capable of improving the prediction horizon in a systematic way. Our results provide an effective methodology for the selection of the future horizon in the development of prediction algorithms for diseases experiencing symptomatic crises.

Conflicts of Interest

The authors declare no conflict of interest.

References

[1] L. Schwiebert, S. K. Gupta, J. Weinmann, Research challenges in wireless networks of biomedical sensors, in: Proceedings of the 7th annual international conference on Mobile computing and networking, ACM, 2001, pp. 151–165.

[2] H. Alemdar, C. Ersoy, Wireless sensor networks for healthcare: A survey, Computer Networks 54 (15) (2010) 2688–2710.

[3] P. Kugler, D. Schuldhaus, U. Jensen, B. Eskofier, Mobile recording system for sport applications, in: Proceedings of the 8th international symposium on computer science in sport (IACSS 2011), Liverpool, 2011, pp. 67–70.

[4] H. Banaee, M. U. Ahmed, A. Loutfi, Data mining for wearable sensors in health monitoring systems: a review of recent trends and challenges, Sensors 13 (12) (2013) 17472–17500.

[5] B. E. Heldberg, T. Kautz, H. Leutheuser, R. Hopfengartner, B. S. Kasper, B. M. Eskofier, Using wearable sensors for semiology-independent seizure detection-towards ambulatory monitoring of epilepsy, in: Engineering in Medicine and Biology Society (EMBC), 2015 37th Annual International Conference of the IEEE, IEEE, 2015, pp. 5593–5596.

[6] C. S. Kutur, K. Ravi Kanth, K. Sree Kanth, Improved algorithm for prediction of heart disease using case based reasoning technique on non-binary datasets, IJRCCT 1 (7) (2012) 420–424.

[7] J. M. Racosta, K. Kimpinski, S. A. Morrow, M. Kremenchutzky, Autonomic dysfunction in multiple sclerosis, Autonomic Neuroscience 193 (2015) 1–6.

[8] H. Kaufmann, D. S. Goldstein, Autonomic dysfunction in parkinson disease, Handb Clin Neurol 117 (2013) 259–278.

[9] A. Boiardi, L. Munari, I. Milanesi, C. Paggetta, E. Lamperti, G. Bussone, Impaired cardiovascular reflexes in cluster headache and migraine patients: evidence for an autonomic dysfunction, Headache: The Journal of Head and Face Pain 28 (6) (1988) 417–422.

[10] B. Babusiak, J. Mohylova, The eeg signal prediction by using neural network, Advances in Electrical and Electronic Engineering 7 (1-2) (2011) 342–345.

[11] P. Goadsby, G. Zanchin, G. Geraud, N. De Klippel, S. Diaz-Insa, H. Gobel, L. Cunha, N. Ivanoff, M. Falques, J. Fortea, Early vs. non-early intervention in acute migraine—'act when mild (awm)'. a double-blind, placebo-controlled trial of almotriptan, Cephalalgia 28 (4) (2008) 383–391.

[12] X. H. Hu, N. H. Raskin, R. Cowan, L. E. Markson, M. L. Berger, U. S. M. S. P. U. Group, et al., Treatment of migraine with rizatriptan: when to take the medication, Headache: The Journal of Head and Face Pain 42 (1) (2002) 16–20.

[13] G. Huang, Y. Zhang, J. Cao, M. Steyn, K. Taraporewalla, Online mining abnormal period patterns from multiple medical sensor data streams, World Wide Web (2013) 1–19.

[14] H. J. Hassinger, E. M. Semenchuk, W. H. O'Brien, Cardiovascular responses to pain and stress in migraine, Headache: The Journal of Head and Face Pain 39 (9) (1999) 605–615.

[15] C. Vollono, V. Gnoni, E. Testani, S. Dittoni, A. Losurdo, S. Colicchio, C. Di Blasi, S. Mazza, B. Farina, G. Della Marca, Heart rate variability in sleep-related migraine without aura, Journal of clinical sleep medicine: JCSM: official publication of the American Academy of Sleep Medicine 9 (7) (2013) 707.

[16] D. Kewman, A. H. Roberts, Skin temperature biofeedback and migraine headaches, Biofeedback and Self-Regulation 5 (3) (1980) 327–345.

[17] J. Pagán, M. I. De Orbe, A. Gago, M. Sobrado, J. L. Risco-Martín, J. V. Mora, J. M. Moya, J. L. Ayala, Robust and accurate modeling approaches for migraine per-patient prediction from ambulatory data, Sensors 15 (7) (2015) 15419. doi:10.3390/s150715419.

[18] J. Passchier, P. Goudswaard, J. F. Orlebeke, Abnormal extracranial vasomotor response in migraine sufferers to real-life stress, Journal of psychosomatic research 37 (4) (1993) 405–414.

[19] C. Lovati, et al., Breathing Sleep Disturbances and Migraine: A Dangerous Synergy or a Favorable Antagonism?, 2012.

[20] PLUX, PLUX-Wireless Biosignlas website, http://www.biosignalsplux.com/index.php/en/, accessed: 2015-07-20.

[21] Nonin, Nonin website, http://www.nonin.com/Home, accessed: 2015-07-20.

[22] K. M. Kellogg, R. J. Fairbanks, A. B. O'Connor, C. O. Davis, M. N. Shah, Association of pain score documentation and analgesic use in a pediatric emergency department, Pediatric emergency care 28 (12) (2012) 1287–1292.

[23] C. E. Rasmussen, C. K. I. Williams, Gaussian Processes for Machine Learning (Adaptive Computation and Machine Learning), The MIT Press, 2005.

[24] C. E. Rasmussen, H. Nickisch, The gaussian processes web site, http://gaussianprocess.org/gpml/code, accessed: 2015-07-20.

[25] R. Burstein, R. Noseda, D. Borsook, Migraine: Multiple processes, complex pathophysiology, The Journal of Neuroscience 35 (17) (2015) 6619–6629.

[26] P. Van Overschee, B. De Moor, N4sid: Subspace algorithms for the identification of combined deterministic-stochastic systems, Automatica 30 (1) (1994) 75–93.

[27] M. Cescon, Modeling and prediction in diabetes physiology, Ph.D. thesis, Lund University (2013).

[28] A. Facchinetti, S. D. Favero, G. Sparacino, C. Cobelli, Detecting failures of the glucose sensor-insulin pump system: improved overnight safety monitoring for type-1 diabetes, in: Engineering in Medicine and Biology Society, EMBC, 2011 Annual International Conference of the IEEE, IEEE, 2011, pp. 4947–4950.

[29] W.-Y. Tan, Z. Ye, Estimation of hiv infection and incubation via state space models, Mathematical biosciences 167 (1) (2000) 31–50.

[30] G. Hooker, S. P. Ellner, L. D. V. Roditi, D. J. Earn, Parameterizing state–space models for infectious disease dynamics by generalized profiling: measles in ontario, Journal of The Royal Society Interface (2010) rsif20100412.

[31] E. Munevar, J. Ramos, W. Gordon, M. Agnew, W. Zhou, Detection of abnormalities in the signal averaged electrocardiogram: a subspace system identification approach, in: Decision and Control, 1999. Proceedings of the 38th IEEE Conference on, Vol. 5, IEEE, 1999, pp. 5094–5099.

[32] Matlab, System Identification Toolbox, V7.14.0.739 (R2012a), The MathWorks Inc., Natick, Massachusetts, 2010.

[33] K. M. Hangos, R. Lakner, M. Gerzson, Intelligent Control Systems: An Introduction with Examples, Springer Science & Business Media, 2001.